Special Section on Pharmacokinetics and ADME of Biological Therapeutics–Minireview

Mathematical Models to Characterize the Absorption, Distribution, Metabolism, and Excretion of Protein Therapeutics

Shufang Liu and Dhaval K. Shah

Department of Pharmaceutical Sciences, School of Pharmacy and Pharmaceutical Sciences, The State University of New York at Buffalo, Buffalo, New York

ABSTRACT

Therapeutic proteins (TPs) have ranked among the most important and fastest-growing classes of drugs in the clinic, yet the development of successful TPs is often limited by unsatisfactory efficacy. Understanding pharmacokinetic (PK) characteristics of TPs is key to achieving sufficient and prolonged exposure at the site of action, which is a prerequisite for eliciting desired pharmacological effects. PK modeling represents a powerful tool to investigate factors governing in vivo disposition of TPs. In this mini-review, we discuss many state-of-the-art models that recapitulate critical processes in each of the absorption, distribution, metabolism/catabolism, and excretion pathways of TPs, which can be integrated into the physiologically-based pharmacokinetic framework. Additionally, we provide our perspectives on current opportunities and challenges for evolving the PK models to accelerate the discovery and development of safe and efficacious TPs.

SIGNIFICANCE STATEMENT

This minireview provides an overview of mechanistic pharmacokinetic (PK) models developed to characterize absorption, distribution, metabolism, and elimination (ADME) properties of therapeutic proteins (TPs), which can support model-informed discovery and development of TPs. As the next-generation of TPs with diverse physicochemical properties and mechanism-of-action are being developed rapidly, there is an urgent need to better understand the determinants for the ADME of TPs and evolve existing platform PK models to facilitate successful bench-to-bedside translation of these promising drug molecules.

Introduction

With the development of the recombinant DNA technology, therapeutic proteins (TPs) have revolutionized treatments for a multitude of diseases and steadily accounted for 50%–60% of the top 10 best-selling drugs worldwide in recent years (Urquhart, 2021). Marketed TPs encompass monoclonal antibodies (mAbs), antibody fragments, enzymes, hormones, growth factors, cytokines, fragment crystallizable (Fc)-fusion proteins, and antibody-drug conjugates (ADCs) (Lagasse et al., 2017). MAbs represent the dominant and the fastest-growing class of TPs in the pipeline, with the 100th mAb approved just recently (Mullard, 2021).

Despite their therapeutic potential, TPs have low success rates in clinical development, with only about 1 in 10 molecules in phase 1 studies approved by the US Food and Drug Administration (Hay et al., 2014). This has been largely attributed to the failure to show significant improvement in the efficacy compared with the placebo group or existing treatments at the clinically tolerated doses of TPs (Arrowsmith, 2011). Although target validation for the chosen indications is vital for the success of TPs (Morgan et al., 2012), sufficient drug exposure at the site of action is a prerequisite for eliciting desired pharmacodynamic (PD) effects, which underscores the importance of understanding the pharmacokinetic (PK) characteristics of TPs. Previous experience with the development of small molecule drugs has suggested that appreciation and research of drug metabolism and PK significantly reduces failures of drug candidates associated with undesired PK characteristics in clinical trials (Kola and Landis, 2004), and we may be witnessing such a transition in the field of TPs as well.

Because of the large size, high polarity, and high affinity of TPs, they differ substantially from traditional small molecule drugs in absorption, distribution, metabolism, and excretion (ADME) pathways (for comprehensive reviews on PK/PD properties of TPs, readers are referred to

ABBREVIATIONS: ABD, albumin binding domain; ADA, antidrug antibody; ADC, antibody-drug conjugate; ADME, absorption, distribution, metabolism, and elimination; BBB, blood-brain barrier; BCSFB, blood-cerebrospinal fluid barrier; CSF, cerebrospinal fluid; Fab, antigen binding fragment; Fc, fragment crystallizable; FcγR, Fc gamma receptor; FcRn, neonatal Fc receptor; GSC, glomerular sieving coefficient; mAb, monoclonal antibody; mPBPK, minimal physiologically based pharmacokinetics; MW, molecular weight; PBPK, physiologically-based pharmacokinetics; PD, pharmacodynamic; PK, pharmacokinetic; PPC, the patches of positive charge; TMDD, target-mediated drug disposition; TfR, transferrin receptor; TP, therapeutic protein.

Lobo et al., 2004; Wang et al., 2008; Vugmeyster et al., 2012; Conner et al., 2020). Unlike many small molecules that display good gastrointestinal absorption, TPs are too large to cross the intestinal membrane and subject to proteolytic degradation in the gut. Therefore, TPs are typically administered via parenteral routes. Distribution of TPs is relatively restricted to the vascular and interstitial spaces, and the tissue concentration is not in rapid equilibrium with that in the plasma. Although small molecule drugs are most commonly eliminated through hepatic metabolism and renal and biliary excretion (Wienkers and Heath, 2005), TPs can be cleared via catabolism in the lysosome following nonspecific pinocytosis or receptor-mediated endocytosis, resulting in small peptides or amino acids that are unlikely to be pharmacologically active or toxic (Shah, 2015). Intracellular catabolism may be circumvented by the interaction between the Fc moiety of TPs and the neonatal Fc receptor (FcRn), which explains the unusually long half-life of mAbs. For TPs with a molecular weight (MW) less than around 60 kDa, renal excretion also represents an important elimination pathway (Meibohm and Zhou, 2012). Nonlinearity in the PK of TPs is not associated with small molecule transporters, metabolic enzymes, or plasma protein binding but frequently attributed to saturable target binding or Fc receptor binding (Ferl et al., 2016).

The distinct ADME features of TPs have aroused many mathematical models to characterize the PK of these molecules. In fact, PK modeling is integral to the drug development and clinical applications of TPs as it supports candidate selection and guides protein engineering strategies in the discovery phase and facilitates clinical translation and optimization of dosing regimens in the clinic. In this mini-review, we provide a brief overview of the PK models that can simultaneously characterize ADME processes of TPs and elaborate on mechanistic submodels that can characterize key distribution, elimination, and absorption processes for TPs. Additionally, we conclude with a discussion on outstanding challenges for modeling the PK of TPs.

Types of PK Models to Characterize the ADME Processes of TPs

The most parsimonious PK model for TPs may be a classic two-compartment model with linear and/or nonlinear clearance. This model appears adequate for recapitulating PK profiles of TPs on many occasions, despite that the assumption underlying the mammillary models (i.e., the elimination of the drug only occurs from the central compartment) does not hold for the majority of TPs. This data-driven model mainly finds use in population PK analysis (Ng et al., 2005) or in PK/PD modeling when the plasma PK is used to drive the PD model (Gibiansky and Frey, 2012).

On the other hand, physiologically-based pharmacokinetic (PBPK) models represent the most complex and mechanistic mathematical framework to characterize ADME of TPs. A typical PBPK model consists of compartments representing various organs connected via blood and lymphatic flows in an anatomic manner (Fig. 1A). Each organ is further divided into vascular, endosomal, interstitial, and cellular spaces, where TP disposition is explicitly defined using physiologic processes as building blocks. PBPK models offer significant advantages over compartmental models. They yield TP concentrations and receptor occupancy in specific organs, allowing the development of reliable exposure-efficacy and exposure-toxicity relationships. The
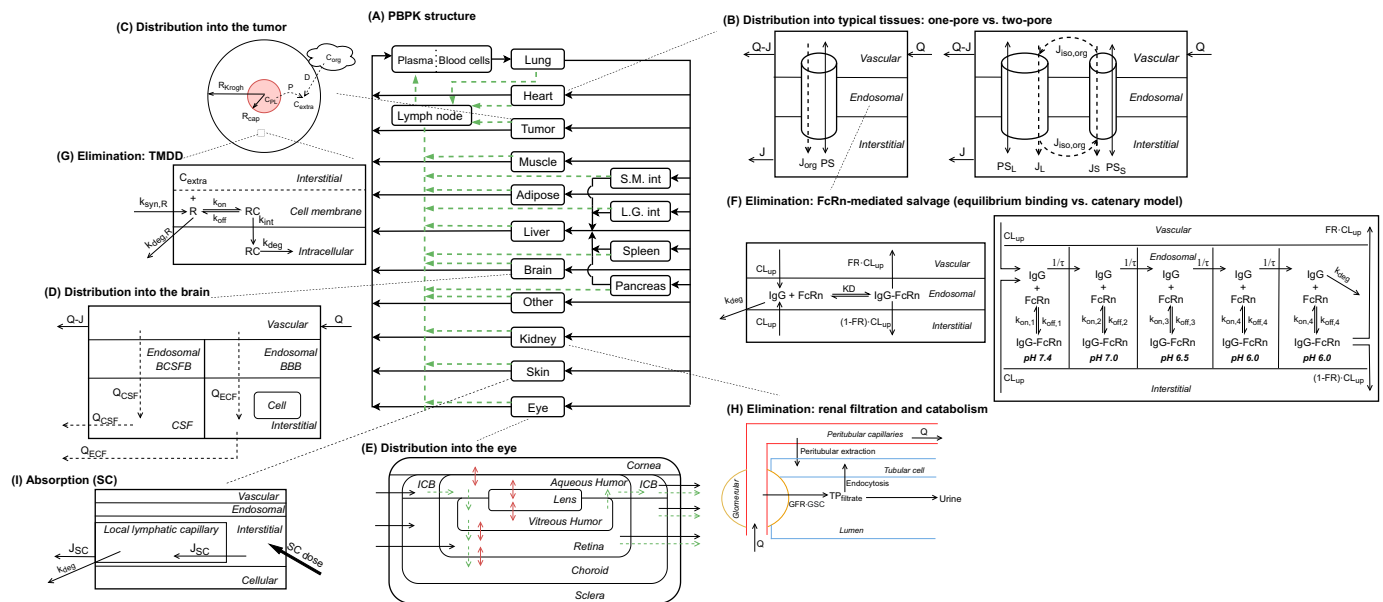
Fig. 1. Schematic of ADME models for TPs. (A) Structure of a whole-body PBPK model for TPs' disposition (adapted from Shah and Betts, 2012). Organs are represented by rectangular compartments connected via blood flows (solid arrows) and lymphatic flows (dashed arrows). Organ-specific distribution or elimination mechanisms will be elaborated below for tumor, brain, eye, kidney, and skin. (B) Diagram of tissue-level models that characterize distribution of TPs for a typical organ (adapted from Sepp et al., 2019), based on one-pore (left panel) or two-pore (right panel) theories. A tissue is divided into vascular, endosomal, and interstitial spaces. Diffusion is denoted by solid arrows and convection by dashed arrows. Specially curved arrows stand for the isogravimetric flow. (C) Representation of the Krogh cylinder tumor model (adapted from Cilliers et al., 2016). The area in red refers to tumoral vasculature, from where TPs can escape via diffusion. Transport of TPs can also be driven by surface uptake from an adjacent organ. (D) Structure of the brain PBPK model. Brain is divided into vascular, BCSFB, BBB, CSF, and parenchymal compartments. (E) Structure of the ocular PBPK model. Regions in the eye include cornea, ICB, lens, retina, choroid, sclera, aqueous humor, and vitreous humor. Black solid arrows represent blood flows, green dashed arrows represent convective flows, and red double-headed arrows represent diffusion processes. (F) Representation of endosomal models that characterize FcRn interaction with IgGs (adapted from Chen and Balthasar, 2012). The panel on the left-hand side assumes equilibrium binding between IgGs and FcRn. The panel on the right-hand side adopts a catenary model, where endosomal subcompartments have pH ranging from 7.4 to 6.0. (G) Representation of a TMDD model for a membrane-bound antigen in the tumor compartment. The free receptor has its inherent turnover rate and is allowed to bind to TPs in the extracellular space of a solid tumor. (H) Schematic of renal elimination of TPs (adapted from Rabkin and Dahl, 1993). Following glomerular filtration, TPs are internalized into tubular cells for degradation or eliminated into the urine. TPs in the postglomerular peritubular capillaries can also be endocytosed, followed by intracellular degradation. (I) Structure of a SC absorption model (adapted from Hu and D'Argenio, 2020). ICB, iris-ciliary body; L.G., int large intestine; SC, subcutaneous; S.M., small intestine.

physiologic nature of PBPK models also enables robust and reliable interspecies scaling and prediction of PK, which is sometimes challenging using traditional allometric scaling as different species have different target expression profiles, target binding, and FcRn binding affinities. Since the development of the first PBPK model for mAbs and antibody fragments by Covell et al. (1986), PBPK models have evolved and expanded to incorporate up-to-date knowledge of physiology and TPs' disposition characteristics. These include molecular size-dependent distribution and elimination (Baxter et al., 1994), target turnover and binding (Baxter et al., 1994), FcRn-mediated recycling (Ferl et al., 2005; Garg and Balthasar, 2007), and interspecies scaling (Baxter et al., 1995; Shah and Betts, 2012). One should be aware that many physiologic parameter values used for various species are collected from diverse resources or scaled/assumed (Shah and Betts, 2012). Boswell and colleagues published a series of work that measured organ vascular and interstitial volumes, and organ blood flow rates for rodents and monkeys, using consistent experimental techniques (Boswell et al., 2011; Boswell et al., 2014; Mandikian et al., 2018). It would be of importance to evaluate how these different physiologic parameter values impact the performance of TP PBPK models.

One way to get around the complex parameterization of a full PBPK model is to employ a minimal PBPK (mPBPK) model, in which tissues are lumped into tight (muscle, skin, adipose, and brain) or leaky (other tissues) compartments based on vasculature and permeability, and the major distribution/elimination pathways are grouped accordingly (Cao et al., 2013). This simplified model still provides physiologically meaningful parameters when only plasma data are available and also has the potential of delineating disposition in tissues of interest by separating out a specific tissue compartment (Chen et al., 2018).

Going forward in this manuscript, we will highlight various models describing ADME processes of TPs, mostly in the context of the PBPK framework, as these models provide the most in-depth and accurate representations of underlying mechanisms and can be readily embedded into a mPBPK framework or linked to a compartmental model after simplification.

Models to Characterize Distribution of TPs

Transcapillary Transport: One-Pore Versus Two-Pore. Although small molecules can enter tissues readily via processes like transcellular diffusion and transporter-mediated uptake, extravasation of TPs is mostly restricted to diffusion and convection through paracellular pores of vascular endothelial wall (Fig. 1B). This process can be mathematically formulated as (Bresler and Groome, 1981):

$$Flux = J_{org} \cdot (1 - \sigma_V) \cdot \frac{\left(C_{org}^V + C_{org}^{IS} \right)}{2} + PS \cdot \left(C_{org}^V - C_{org}^{IS} \right) \quad (1)$$

Where J_{org} is the organ lymph flow, C_{org}^V and C_{org}^{IS} are vascular and interstitial concentrations of a tissue, and PS is the permeability-surface area product. σ_V is the tissue vascular reflection coefficient, which represents the fraction of a solute that is unable to cross the pores. Typically, σ_V is greater (i.e., higher resistance) for larger-size proteins (Covell et al., 1986) and tissues with less leaky vasculature (Shah and Betts, 2012). For TPs as large as mAbs (150 kDa), the transcapillary transport is considered almost entirely convective (Baxter et al., 1995), and thus the flux from vascular space to interstitial space can be reduced to $J_{org} \cdot (1 - \sigma_V) \cdot C_{org}^V$. Similarly, the mass transport from interstitial fluid to lymphatics is described as $J_{org} \cdot (1 - \sigma_I) \cdot C_{org}^{IS}$, where σ_I is the lymphatic reflection coefficient. One crucial assumption underlying these equations is that the pores have a uniform size (homoporosity, or one-pore model), which contradicts the actual physiology.

The two-pore phenomenon was first noted in the 1950s (Grotte, 1956) and further elaborated and mathematically formulated by Rippe and Haraldsson (1987, 1994). Continuous and fenestrated endothelium is assumed to contain two categories of pores, small pores (radius $r_s = 4.44$ nm) and large pores (radius $r_L = 22.85$ nm), and protein solutes extravasate by diffusion or convection via both types of pores (Fig. 1B). What makes the two-pore framework distinct from the one-pore model is the incorporation of isogravimetric flow (J_{iso}), a circulation flow entering large pores and existing small pores, which can explain a transvascular flux of proteins even in the absence of net filtration ("isogravimetric" state). Accordingly, the actual lymph flows through these pores corrected for J_{iso} are:

$$J_{L,org} = J_{iso,org} + \alpha_L \cdot J_{org} \quad (2)$$

$$J_{S,org} = -J_{iso,org} + \alpha_S \cdot J_{org} \quad (3)$$

Where $J_{L,org}$ and $J_{S,org}$ are organ lymph flows through large and small pores, α_L and α_S are relative abundance of both pores, and J_{org} is the net organ lymph flow. Thus, both diffusive and convective processes for protein extravasation can be characterized in the clearance terms as below:

$$CL_{tp,\ L,\ org} = PS_{L,org} \left(1 - \frac{C_{org}^{IS}}{C_{org}^V} \right) \frac{Pe_{L,\ org}}{e^{Pe_{L,\ org}} - 1} + J_{L,org}(1 - \sigma_L) \quad (4)$$

$$CL_{tp,\ S,\ org} = PS_{S,org} \left(1 - \frac{C_{org}^{IS}}{C_{org}^V} \right) \frac{Pe_{S,\ org}}{e^{Pe_{S,\ org}} - 1} + J_{S,org}(1 - \sigma_S) \quad (5)$$

$CL_{tp,L,org}$ and $CL_{tp,S,org}$ are transcapillary clearances through large and small pores in an organ, $PS_{L,org}$ and $PS_{S,org}$ are the permeability-surface area products, and σ_L and σ_S are vascular reflection coefficients. Particularly, $Pe_{L,org}$ and $Pe_{S,org}$ are the Peclet numbers that reflect the importance of convection versus diffusion in the extravasation process and defined as:

$$Pe_{L,org} = \frac{J_{L,\ org}(1 - \sigma_L)}{PS_{L,org}} \quad (6)$$

$$Pe_{S,org} = \frac{J_{S,\ org}(1 - \sigma_S)}{PS_{S,org}} \quad (7)$$

The two-pore formalism has been applied in PBPK models developed for antibodies and antibody fragments since 1994 (Baxter et al., 1994). Early work typically estimated values of certain key parameters, such as PS, Pe, J_{iso}, and σ (Baxter et al., 1994; Ferl et al., 2005; Davda et al., 2008) as they are difficult to measure and can vary depending on drugs and organs. Unfortunately, these parameter estimates differ substantially between studies and are often associated with high uncertainty and poor identifiability, restricting extensive utilization of the two-pore model. Sepp et al. mathematically derived $J_{iso,org}$ and PS_{org} and found that they can be expressed as explicit linear functions of J_{org}. Additionally, they also reported that Pe could be calculated using an empirical equation for σ_v (Sepp et al., 2015). Due to these derivations, their model greatly reduced the number of parameters fitted (only J_{org} needed to be estimated for the two-pore extravasation) and could capture the whole-body PK of a nonbinding domain antibody. In pursuit of development of a generalized PBPK model to characterize a diverse array of TPs, Li and Shah (2019) further expressed glomerular sieving coefficient (discussed later), PS_{org}, Pe, and σ as functions of MW so that the two-pore PBPK model could a priori predict the PK of eight TPs of different sizes without fitting any parameter and facilitate a better understanding

of the contribution of diffusion and convection toward protein transport across a wide range of MW.

Special Tissues. In whole-body PBPK models, various tissues are usually treated as modules with similar kinetic processes. However, certain tissues differ significantly in terms of anatomy and physiology (e.g., solid tumor, brain, eye) and may require dedicated PK models for characterization of TP concentrations.

In solid tumors, deficient lymphatic drainage causes high interstitial hydrostatic pressure, which precludes convection of macromolecules. Meanwhile, the capillary wall tends to be more permeable than blood vessels in healthy tissues (Boucher et al., 1990). These features imply that extravasation of TPs is primarily dependent on diffusion. In addition, the solid tumor space can be viewed as a collection of Krogh cylinders, and TP distribution into the tumor can be described as:

$$\frac{dC_{extra}}{dt} = \frac{2PR_{cap}}{R_{Krogh}^2} \cdot \left(C_{PL} - \frac{C_{extra}}{\varepsilon} \right) + \frac{6D}{R_t^2} \cdot \left(C_{org} - \frac{C_{extra}}{\varepsilon} \right) \quad (8)$$

(Thurber et al., 2008; Schmidt and Wittrup, 2009; Thurber and Wittrup, 2012). The first term refers to protein permeation through the vascular capillary, and the second term indicates diffusion-driven uptake from the tumor surface that is in contact with the surrounding tissue (surface uptake), as shown in Fig. 1C. C_{extra}, C_{PL}, and C_{org} represent TP concentrations in the tumor extracellular space, the plasma, and the surrounding tissue. P is the permeability coefficient across the capillary wall, D is the diffusion coefficient, ε is fraction of tumor that is accessible to macromolecules, R_{cap} is the capillary radius, R_{Krogh} is half the average distance between blood vessels within the tumor, and R_t is tumor radius. It is apparent in the equation that the surface uptake pathway dominates when the tumor is small and less vascularized (i.e., small R_t), and the TP distribution occurs almost exclusively from extravasation when the tumor is larger and vasculature is well developed. Schmidt and Wittrup also derived empirical relationships between molecular size and P, D, and ε by fitting a two-pore model of the capillary wall and a two-pore model of tumor interstitium using experimental data (Schmidt and Wittrup, 2009). These relationships not only help readily calculate tumor uptake for various TPs but also provide insights into the antigen binding affinity required for prolonged retention in the tumor for different-size TPs.

In addition to extravasation into the tumor, heterogeneous intratumoral distribution is of great interest. The heterogeneity is often featured by perivascular distribution of TPs, leading to regions of antigen-positive cells completely untargeted. This phenomenon is attributed to the "binding site barrier," which refers to high-affinity binding to the target (and subsequent degradation) right after extravasation of the TP preventing deeper distribution into the tumor (Fujimori et al., 1990). A few model structures have been proposed to delineate heterogeneous drug distribution within a tumor, with different levels of complexities. The Krogh cylinder model in conjunction with a PBPK framework has been capable of predicting antigen-bound fraction as a function of the distance from the vasculature and evaluating strategies to overcome the binding site barrier (Cilliers et al., 2016). Shah et al. proposed a spherical tumor model that contains five circular layers with equal thickness, with adjacent layers connected by permeability surface area coefficients (Shah et al., 2009). This model can be modified to characterize the binding site barrier by incorporating target expression and binding in each tumor layer (Glassman and Balthasar, 2019). The simplest approach is to allow only a fraction of tumor antigens to be accessible for binding (Urva et al., 2010), but the associated caveats are complete loss of information about the heterogeneity and poor generalizability of the fraction term when drug doses, binding affinities, or tumor sizes change.

The brain represents another challenging tissue to model as it is known to have a tight blood-brain barrier (BBB) and blood-cerebrospinal fluid

barrier (BCSFB), and complex fluid flows in the central nervous system. A generic two-pore PBPK model in PK-Sim platform could fit antibody disposition data in mouse brain reasonably well, and the brain lymph flow and hydraulic conductivity were estimated to be extremely low (Niederalt et al., 2018). Adding a cerebrospinal fluid (CSF) flow exiting the brain that removes macromolecules can further reduce predicted brain exposures of TPs (Brinker et al., 2014; Sepp et al., 2019). Change et al. presented a higher spatial-resolution brain PBPK model that details paracellular transport and transcytosis through BCSFB and BBB, CSF compartmentalization (including lateral ventricle, third-fourth ventricle, cisterna magna, and subarachnoid space), and circulations of CSF and brain extracellular flow (Fig. 1D). This translational model was calibrated using rat disposition data in various brain regions and accurately predicted brain PK of mAbs in mice, monkeys, and humans (Chang et al., 2019).

As the research on eye diseases expands, ocular disposition is of more interest. The eye is characterized by delicate compartmentation, a variety of barriers, and complex fluid dynamics (Perez et al., 2013). Intravitreal dosing is the mainstream administration route in treating ocular disorders such as age-related macular degeneration and diabetic retinopathy, which requires frequent injections and causes pain. On the other hand, several anticancer mAbs and ADCs targeting diverse antigens have been shown to induce ocular toxicities following intravenous injections. As such, modeling drug exposures in the eye is valuable not only for prioritizing suitable TPs during drug development and optimization of dosing regimen but also for evaluating ocular toxicity potential. A novel anatomic ocular compartment that contains cornea, iris-ciliary body, aqueous humor, lens, vitreous humor, retina, choroid, and sclera, embedded in a PBPK framework, has been proposed to characterize ocular disposition following intravitreal or systemic administration (Bussing and Shah, 2020), as shown in Fig. 1E. Considering that current antivascular endothelial growth factor TPs for ocular diseases include IgG, Fc-fusion, antigen-binding fragment (Fab), and single-chain variable fragment formats, the two-pore formalism is anticipated to be incorporated in the ocular compartment to better characterize the ocular absorption and disposition processes.

Models to Characterize Catabolism and Excretion of TPs

TPs are typically eliminated by the following pathways: (1) target-mediated drug disposition, (2) nonspecific pinocytosis/endocytosis followed by intracellular catabolism (for larger TPs) throughout the body, (3) renal filtration (for smaller TPs), and (4) antidrug antibody (ADA)-induced clearance. In particular, FcRn-mediated salvage plays an important role in the disposition of mAbs and Fc-fusion proteins.

Interaction with FcRn. FcRn is known to be expressed in vascular endothelial cells of many tissues and hematopoietic cells and contribute to the long serum persistence of IgGs and albumin. Binding between IgGs and FcRn is pH-dependent, with high affinity at acidic pH and negligible binding at physiologic pH. Following fluid phase pinocytosis, IgG binds to FcRn upon acidification of endosomes. Unbound IgG is subject to lysosomal degradation, whereas FcRn-bound IgG is returned to apical or basolateral cell surface. Once exposed to the physiologic pH of extracellular fluid, IgG is released into the systemic circulation or the interstitial fluid.

The PBPK model by Ferl et al. was one of the first to account for FcRn expression in skin and muscle and incorporated IgG uptake into endothelia, IgG binding to FcRn, recycling of FcRn-bound IgG, and degradation of unbound IgG in the endosome (Ferl et al., 2005). The PBPK model proposed by Garg and Balthasar accounted for FcRn expression in all the tissues and characterized mAb PK in wild-type and FcRn-knockout mice (Garg and Balthasar, 2007). As shown in Fig. 1F, they assumed an equilibrium binding between mAb and FcRn in the endosomal space. Therefore,

within the endosomal compartment, unbound IgG was expressed as a fraction (f_u) of total IgG, and f_u was defined as:

$$f_u = 1 - \frac{1}{2 \times C_{Endo,\ org}^{Total}} \times \left(K_D + nPt_{org} + C_{Endo,\ org}^{Total} \right.$$

$$\left. - \sqrt{\left(K_D + nPt_{org} + C_{Endo,\ org}^{Total} \right)^2 - 4 \times C_{Endo,\ org}^{Total} \times nPt_{org}} \right) \quad (9)$$

Above, $C_{Endo,\ org}^{Total}$ is the total endosomal IgG concentration in an organ, nPt_{org} is the total FcRn concentration, and K_D is the dissociation constant of the antibody for binding to FcRn. Compared with the model by Ferl, in this model the organ-specific FcRn capacity was assumed to be proportional to organ weight and adjusted based on total FcRn amount in the body. This model estimated the fraction of FcRn-bound antibody that recycles back to the vascular space (FR) to be 0.715, and this value has been carried forward in many subsequent PBPK models. Nowadays, FcRn-mediated recycling is routinely incorporated within mAb PBPK models, with variable assumptions across models.

Prompted by the fact that the equilibrium binding model over-predicts the improvement in antibody half-life with increasing equilibrium affinity of FcRn binding at pH 6, Chen and Balthasar (2012) constructed a catenary FcRn binding model that describes endosomal transit process, gradual acidification of endosomes, and kinetic binding between the antibody and FcRn. This was justified by the fact that residence time in endosomes (~10.8 minute) is too short for the mAb-FcRn interaction to reach equilibrium (dissociation half-life of 6–58 minute). In this catenary model, the vascular endosomal space is subdivided into five transit compartments with pH of 7.4, 7.0, 6.5, 6.0, and 6.0, and the transit time (τ) was determined to be 2.7 minute through each compartment (Fig. 1F). FcRn was allowed to interact with IgG using pH-dependent association rates (k_{on}^{pH}) and dissociation rates (k_{off}^{pH}) in each subcompartment, and only in the last subcompartment unbound IgG was assumed to be cleared and bound IgG was assumed to recycle. Of note, an underlying constraint between the tissue endosomal subcompartment volume (V_{org}^E) and uptake clearance (CL_{up}^{org}) exists in this model to ensure endosomal volume homeostasis and FcRn and endogenous IgG steady-state:

$$V_{org}^E = CL_{up}^{org} \cdot \tau \quad (10)$$

Additionally, this model employs measured tissue-specific FcRn expression (Li and Balthasar, 2018), contrary to assuming a universal FcRn concentration across tissues in prior models (Urva et al., 2010; Shah and Betts, 2012). The equilibrium binding model performed as well as the catenary model in predicting PK of normal mAbs. However, the former predicts an almost proportional increase in mAb half-life with enhanced FcRn binding, whereas the latter predicts much more modest half-life extension, which is more consistent with observations reported in the literature (Chen and Balthasar, 2012).

In prior models, FcRn concentrations are assumed to be static (either tissue-specific or universal), which makes them inappropriate for characterizing PK of anti-FcRn mAbs used in treating autoimmune diseases as FcRn density is expected to be altered under the treatment. Accordingly, on top of the catenary model, Li and Balthasar (2019) took account of FcRn turnover by supplementing an FcRn pool compartment, where synthesis and degradation of FcRn can occur. This pool compartment provides the first endosomal subcompartment with FcRn and collects unbound and IgG-Fc–bound FcRn from the last endosomal subcompartment at a rate of $\frac{1}{\tau}$. Anti-FcRn mAbs are allowed to bind to FcRn through either the Fab arms or Fc region. In the last subcompartment, Fc-bound mAb is recycled, whereas mAb-FcRn complexes linked via the Fab domain are either degraded or recycled directly to the first

subcompartment. Such model scheme allows characterization of FcRn depletion in the presence of FcRn inhibitors.

There is also a growing interest in the role of hematopoietic cells in mAb PK (Challa et al., 2019; Malik and Edginton, 2020), as FcRn is expressed in these cells (Vidarsson et al., 2006; Latvala et al., 2017), and hematopoietic cells exist ubiquitously in the body (Yu et al., 2016). Experiments involving wild-type and hematopoietic cell-specific FcRn knockout mice have shown that endothelial and hematopoietic cells almost contributed equally to FcRn-mediated salvage (Akilesh et al., 2007; Montoyo et al., 2009; Richter et al., 2018). Correspondingly, the model mentioned above also considers mAb-FcRn interactions in endosomal space associated with hematopoietic cells, which are assumed to reside within the lymph, tissue interstitial space, and plasma (Li and Balthasar, 2019). However, widespread validation of such model remains unaccomplished.

Target-Mediated Drug Disposition. Target-mediated drug disposition (TMDD), a term coined by Levy (1994), refers to situations where high-affinity binding to the target impacts the PK characteristics of the drug. TMDD applies to the majority of TPs as this class of drugs is designed to have high affinity and specificity for their targets. However, its impact on the PK is only noticeable at lower TP concentrations when this pathway is not saturated. TMDD modeling has a history of about 20 years, and many seminal works have been done to establish the mechanistic framework, evaluate the identifiability of model parameters, simplify the model equations, and modify the model to characterize novel molecules. Interested readers are referred to (Mager and Krzyzanski, 2005; Gibiansky et al., 2008; Marathe et al., 2009; Gibiansky and Gibiansky, 2014; Lavezzi et al., 2018; Peletier and Gabrielsson, 2018) for detailed education on this topic. Only a few TMDD models will be highlighted below.

A full, generic TMDD model was proposed by Mager and Jusko (2001). The model assumes that drug in the central compartment (C_p) can distribute into the peripheral compartment (D_T), be cleared in its free form (via the elimination rate k_{el}), or bind (rate constant, k_{on}) to the free target (R) to form the drug-receptor complex (RC). R is produced (via the synthesis rate, k_{syn}) and eliminated (via the degradation rate, k_{deg}) in the central compartment, whereas RC may undergo dissociation (k_{off}) or internalization (k_{int}). For soluble targets, k_{int} is usually close to k_{el} of the free drug. For membrane-bound targets, k_{int} is often similar to k_{deg} of the free receptor, and when this holds, the total receptor concentration (R_{tot}, i.e. $R + RC$) is constant, which eliminates the need to mathematically define temporal changes in R_{tot}. Several approximations of the full TMDD model can be implemented to avoid estimating practically unidentifiable parameters such as k_{on} and k_{off}, and to make the equations less stiff. For example, when k_{on}, k_{off}, and k_{int} are much faster than the remaining processes, it can be assumed that the free drug, the free receptor, and complex are at quasi-steady-state, with $RC = \frac{R_{tot} \cdot C_p}{K_{SS} + C_p}$ at all times, where K_{SS} represents $\frac{k_{off} + k_{int}}{k_{on}}$ (Gibiansky et al., 2008). If k_{int} is much smaller than k_{off}, the assumption of quasi-equilibrium becomes valid, where $RC = \frac{R_{tot} \cdot C_p}{K_D + C_p}$, with K_D being $\frac{k_{off}}{k_{on}}$ (Mager and Krzyzanski, 2005). Furthermore, if $R \ll C_p$, both quasi-steady-state and quasi-equilibrium models can be reduced to Michaelis-Menten approximation (Gibiansky et al., 2008).

PBPK models usually adopt the full, quasi-steady-state, or quasi-equilibrium TMDD component in the tumor compartment (Urva et al., 2010; Shah and Betts, 2012; Cao and Jusko, 2014), using receptor and drug concentrations at the site of action instead of the central compartment (Fig. 1G). Parameters such as R_{tot}, K_D, k_{on}, k_{off}, or even k_{int} to operate these models could be obtained from in vitro measurements. Other physiologically relevant issues also need to be considered by these models, such as tumor antigen accessibility (discussed in

Distribution Models) and antigen shedding. Many membrane-bound targets are known to shed the ectodomains or have a soluble form in the body (Kuang et al., 2010). This circulating pool competes with the cell-surface counterpart for drug binding and alters disposition and efficacy of the TP. A mPBPK-TMDD model incorporating the target-shedding mechanism of human epidermal growth factor receptor 2 (HER2) has systematically evaluated the effects of target shedding kinetics, soluble target turnover, and affinity difference between cell-surface HER2 and shed HER2, on plasma PK of trastuzumab (an anti-HER2 antibody), as well as receptor occupancy of membrane-bound HER2 (Li et al., 2014). Such TMDD model with target shedding was further modified and incorporated into a population PBPK framework to demonstrate the concentration of shed HER2 ectodomain as one of the key factors that contribute toward interindividual variability in trastuzumab PK (Malik et al., 2017).

Renal Elimination. Kidney contributes to both catabolism and excretion of TPs. Renal excretion is a highly size-dependent process, and therefore is an important determinant of PK differences observed for TPs across a wide MW range. The molecular size cutoff for glomerular filtration is approximately 60 kD, and an inverse sigmoidal relationship between glomerular sieving coefficient (GSC) and MW has been demonstrated (Haraldsson et al., 2008). The size selectivity makes the renal filtration process fit well with the two-pore model, where GSCs can be expressed as empirical functions of MW (Li and Shah, 2019; Sepp et al., 2019). A pathway analysis reveals that lysosomal catabolism dominates the elimination of TPs with MW greater than 100 kD, and TPs less than 100 kDa are mostly eliminated via renal filtration (Li and Shah, 2019). In addition to size, other TP-specific factors also play a role in glomerular filtration. A positive correlation between GSC and molecular charge was also observed, which is attributed to the negatively charged glycocalyx of the filtration barrier (Haraldsson et al., 2008). A recent study reveals that renal filtration is higher for one-armed (nonbranched) IgGs and IgGs with a more flexible hinge region (Rafidi et al., 2021). More quantitative data on systemic and kidney PK of TPs are needed to incorporate factors such as charge, shape, and rigidity as covariates in PK models. Similar to other organs, renal endothelial cells can take up TPs for lysosomal degradation. Additionally, renal catabolism can occur via reabsorption into endocytic vesicles of proximal tubule cells following glomerular filtration or by peritubular extraction of TPs from postglomerular capillaries (Meibohm and Zhou, 2012), as shown in Fig. 1H. However, these catabolism mechanisms have not been explicitly accounted for in most current models.

Immunogenicity. TPs with antigenic components, such as foreign sequences and impurities, can induce immunogenicity and ADA formation. Although in rare cases ADAs serve as a storage depot that sustains TP exposures (Wang et al., 2008), they often compromise drug PK to varying degrees, depending on ADA titer, kinetics, and types (neutralizing or non-neutralizing).

Empirical models with time-varying PK parameters have been used to study the impact of immunogenicity on PK of TPs. For example, a parameter termed change in clearance time (α) was included in a two-compartment TMDD model, which allows the linear clearance to suddenly change at time α, presumably due to ADA formation (Kathman et al., 2016). It was found that the derived α can be much earlier than the time when ADA is detected in bioassays and thus is helpful in identifying false-negative subjects. Certain more mechanistic models introduce a compartment representing ADA depot that is activated by repeated dosing of TPs, and after some transit time, ADAs are available in the central compartment to bind to TPs and get eliminated (Chen et al., 2013; Perez Ruixo et al., 2013). The dissociation rate of ADAs binding to TPs can decay over time to reflect affinity maturation (Chen et al., 2013).

These models are useful to determine the onset and magnitude of influence of ADA on TP disposition but cannot project immunogenicity based on in vitro and preclinical data. To aid the immunogenicity risk assessment during drug development, Chen et al. (2014a, 2014b) proposed a mechanistic, multiscale, prototype framework that integrates subcellular, cellular, and whole-body level models. The subcellular model focuses on antigen presentation processes, including activation of dendritic cells by endotoxin existent in TP formulations, internalization of the antigenic TP, degradation of the TP into T-cell epitope peptides, binding between peptides and major histocompatibility complex class II molecules, and presentation of T-epitope-MHC complexes on dendritic cell membrane. The cellular model further recapitulates activation, proliferation, and differentiation of T helper cells and B cells, which ultimately results in the secretion of ADAs from plasma cells. Total 17 subgroups of B cells and derived ADAs are assumed with incremental binding affinities to the antigenic TP so that the affinity maturation can be captured. The differential equation–based subcellular and cellular models are readily integrated with an extended two-compartment model to describe in vivo disposition of ADAs and the TP. Modeling the impact of immunogenicity on PK is achieved by adding the following two components to the clearance of TP: (1) rapid elimination of ADA-TP immune complex and (2) internalization of TP following B-cell receptor binding. Of note, such mechanistic modeling allows for incorporating drug-specific, product-specific, and patient-specific characteristics and can generate predictions of immunogenicity incidence and its influence on PK of TPs in a given population.

Models to Characterize TP Absorption

Due to the presence of proteolytic enzymes in the gastrointestinal tract, TPs are frequently administered via parenteral routes, such as intravenous, subcutaneous, and intramuscular delivery. subcutaneous administration has been approved for the delivery of many TPs as it is the most convenient route for chronic treatments and enables drug delivery for prolonged periods of time (McDonald et al., 2010). Subcutaneous dosing refers to injections into the hypodermis (interstitial space), from where TPs can gain access to the systemic circulation, via diffusion through blood capillaries (for TPs with MW <16 Kd) or convection through the lymphatic vessels (for TPs with MW >16 kD) that drain into the blood. For molecular modalities with Fc, FcRn-mediated transcytosis serves as an important pathway for the subcutaneous absorption (Deng et al., 2012; Richter and Jacobsen, 2014).

To model the absorption of TPs, an absorption site compartment can be linked to the central/plasma compartment via some absorption rate constants; the bioavailability can be explicitly expressed as F or reflected in a first-order degradation process from the subcutaneous site. Readers are referred to the review (Kagan, 2014) that describes applications of such empirical and semimechanistic models in characterizing subcutaneous absorption of diverse TPs, and physiologic interpretations of relevant parameters. In the PBPK framework, the subcutaneous site is often considered as a typical tissue compartment with vascular, endosomal, interstitial (i.e., the injection site), and cellular space. An extra clearance term is allowed either in the interstitial space or in the local lymphatic capillary to represent presystemic catabolism that occurs outside vascular endothelia, as shown in Fig. 1I (Porter and Charman, 2000).

Many physiologic factors such as FcRn expression, lymphatic vessel density and lymph flow rates, extracellular matrix, and injection sites, together with physicochemical properties of TPs such as MW, charge, aggregation potential, and immunogenicity, are known to influence PK following subcutaneous administration (Sanchez-Felix et al., 2020). Mechanistic models have been used to mathematically describe the interplay of these factors and to investigate their impacts on the extent

and rate of subcutaneous absorption. Sensitivity analysis done in various models has revealed that T_{max} is most sensitive to lymphatic flow rate, whereas bioavailability is significantly impacted by lymphatic transit time, degradation during lymphatic transport, FcRn expression, and FcRn binding affinity (Zhao et al., 2013; Kagan, 2014). To mechanistically understand the effect of molecular size on subcutaneous absorption, a two-pore formalism can be applied in the subcutaneous site (Ibrahim et al., 2012; Gill et al., 2016; Hu and D'Argenio, 2020; Li et al., 2021), as discussed in *Distribution Models*. Pathway analysis using such two-pore models suggests that percentage of presystemic degradation increased with increasing MW of proteins, with the exception of mAbs due to FcRn-mediated protection, and that the fraction absorbed through lymphatic transportation becomes more prominent for larger-size TPs (Gill et al., 2016; Li et al., 2021). Positive charge patches on TPs are believed to interact with abundant hyaluronic acid, the highly negatively charged polysaccharides in subcutaneous space, which hinders the movement of molecules in the interstitium (Reddy et al., 2006; Mach et al., 2011). Correspondingly, proteins with higher pIs showed delayed T_{max} in lymph and reduced subcutaneous bioavailability (Reddy et al., 2006; Zheng et al., 2012). A two-pore PBPK model that intended to a priori predict human plasma PK of different-size TPs following subcutaneous failed to see any correlation between prediction accuracy of C_{max} or T_{max} and TP pIs (Gill et al., 2016). In contrast, another two-pore PBPK model that allowed flexibility in subcutaneous lymphatic capillary clearance for 12 antibodies found a positive correlation between the parameter estimates and the positive charge in complementarity-determining regions (Hu and D'Argenio, 2020). Richer data from more TPs and a wider range of pI/charge are needed to validate and refine such correlations derived from the PBPK models.

All the above-mentioned models can capture experimental data reasonably well, but their interspecies translatability and physiologic relevance remain questionable. It is well recognized that prediction of subcutaneous absorption in humans based on data from preclinical species is very difficult (Collins et al., 2020), which is largely attributed to interspecies differences in skin physiology (e.g., panniculus carnosus muscle is present in lower species but absent in humans) (Richter and Jacobsen, 2014), FcRn interactions (Ober et al., 2001), and relative contribution of lymphatics to the absorption (e.g., lymphatic absorption is important to subcutaneous bioavailability in sheep but less so in rodents) (Porter et al., 2001; Kagan et al., 2007). To our knowledge, traditional empirical models in conjugation with allometric scaling and mechanistic PBPK models do not seem to be capable of taking into account these complexities and robustly projecting bioavailability across species. In addition, it has been suggested that FcRn-mediated protection of mAbs in hematopoietic cells is important to subcutaneous bioavailability as the bioavailability was greatly compromised when FcRn was absent only in hematopoietic cells (Richter et al., 2018). The importance of this absorption mechanism needs to be thoroughly evaluated via modeling approaches.

Despite the predominant role of subcutaneous dosing in clinical TP therapies, other administration routes of TPs are gaining attention. Among them, noninvasive pulmonary delivery is experiencing renewed interest in view of the outbreak of COVID-19. Two marketed inhaled TPs, rhDNase I (Pulmozyme) and insulin (Afrezza), represent locally and systemically acting biologics via pulmonary entry, respectively. More than 25 inhaled TPs are being evaluated in clinical trials, targeting cystic fibrosis, asthma, and respiratory viral infections including COVID-19 (Liang et al., 2020). Pulmonary delivery takes advantage of the large surface area, extensive vasculature, relatively low proteolytic enzyme activity, and high permeability in the lung (Chung et al., 2012), with the potential to achieve rapid absorption for systemic delivery (Patton and Byron, 2007) and high local concentrations for topical therapy.

Meanwhile, it faces challenges such as branching lung structures as barriers for deposition, limited fluid volume for particle dissolution (Patton et al., 2010), and rapid mucociliary and macrophage clearance. Therefore, mathematical lung submodels that incorporate salient anatomic features, spatial distribution of FcRn, fluid dynamics, protein transportation kinetics, and mucociliary clearance would be helpful in quantitative understanding of mechanisms underlying pulmonary absorption and guiding strategies to optimize TPs for inhalation. A multicompartment lung PBPK model originally intended for small molecules can serve as a starting template (Gaohua et al., 2015) and be further expanded to depict macromolecule-relevant processes.

Opportunities and Challenges

All the PK models for TPs described above have some advantages and disadvantages associated with them, which have been summarized in Table 1. Depending on their applicability, different models are frequently used in mechanistic preclinical studies and clinical settings to expedite drug discovery and development process (Glassman and Balthasar, 2019; Gibbs et al., 2020). The ultimate goal of investigating and modeling PK of TPs is to translate preclinical findings into humans and facilitate first-in-human dose selection and optimization of clinical dosing regimens. There is currently no consensus on the best way for interspecies scaling of TPs' PK (Germovsek et al., 2021). Nonetheless, multiple attempts have been made to validate the capability of PK models to predict human PK from preclinical species or to extrapolate from human adults to pediatric populations, as listed in Table 2. Although detailed discussion of this topic is beyond the scope of this mini-review, cross-species and crosspopulation prediction of TPs' PK is a promising and rapidly growing area. Going forward, more work needs to be done to reveal physiologic differences between species or populations that may impact ADME of TPs and to demonstrate general applicability of such PK models for a diverse array of TPs under different pathologic conditions. In this section, we have further discussed additional opportunities and challenges that PK scientists may face while developing mathematical models to characterize ADME of TPs.

Interantibody Differences in PK. The most prominent feature that distinguishes diverse TPs is the MW range (3.5 kDa to 150 kDa) and the size-dependent ADME mechanisms have been decently characterized using two-pore models. Nonetheless, mAbs with MW of around 150 kDa can still display very distinct PK profiles, even in cases where FcRn affinities are similar and TMDD is absent. Other key factors that are known to govern ADME properties of mAbs include charge, glycosylation, and shape, and some emerging models have attempted to address their influences on mAb PK.

Chen and Balthasar (2012) suggested two coefficients, $F1$ and $F2$, that can be applied to modify the endosomal uptake clearance ($F1 \cdot CL_{up}$) and transcapillary convection ($F2 \cdot (1 - \sigma_v)$), respectively, to account for interantibody variability in PK (Glassman et al., 2015). Using a similar yet augmented approach, Hu and D'Argenio (2020) applied four mAb-specific parameters in a PBPK model that represent antibody variabilities in the pinocytosis rate (S_{pino}), diffusive/convective transport rates ($S_{diff-conv}$), and lymphatic capillary uptake rate (S_{LymUpt}^{SC}) and presystemic clearance (CL_{LymUpt}^{SC}) following subcutaneous dosing to individually fit intravenous and subcutaneous PK data of many mAbs in the training dataset. It was found that parameter estimates of both S_{pino} and CL_{LymUpt}^{SC} positively correlated with positive charges of the complementarity-determining region vicinity (PPC), consistent with the observations that increased positive charges of mAbs lead to enhanced cellular uptake and lower bioavailability (Bumbaca Yadav et al., 2015; Datta-Mannan et al., 2015). When these two relationships based on PPC were incorporated in the model, they

TABLE 1

Summary and characteristics of various PK models for TPs

	Advantages	Disadvantages
ADME Models		
Compartmental	• Easy to implement • Minimal number of parameters • Sufficient to link to basic PD models	• The mammalian model assumption does not apply to TPs • Vague biologic interpretation of parameters • Lack translatability across species for nonlinear PK
Minimal PBPK	• Easier than full PBPK to implement • Parameters are biologically relevant • Sufficient when only few organs are of interest	• Unable to reflect processes in all the organs
Full PBPK	• Reflect concentrations in most organs and site of action • Parameters are physiologically meaningful • Suitable for interspecies scaling	• Relatively complicated to code • Low model running speed • Less confidence in certain parameter values
Distribution Models		
One-pore	• Sufficient to describe TPs of the same size	• Unable to serve as a platform to describe various-size TPs
Two-pore	• More physiologically relevant • Can serve as a platform model for TPs of different sizes	• Relatively complicated • Predictability may be compromised for certain-sized TPs
FcRn Models		
Equilibrium	• Sufficient to describe wildtype Fc when k_{off} is large • Eliminate the parameter identifiability issue	• Inappropriate for TPs exhibiting a dissociation half-life longer than endosomal trafficking time (e.g., engineered FcRn binders)
Kinetic binding	• Suitable for TPs even when binding equilibrium is not reached in endosomes • Allows investigation of differential effects of k_{on} and k_{off}	• Model stiffness • Unable to capture differential binding at gradually changed pH
Catenary model	• Gradual acidification and trafficking time in endosomes make the scenarios more realistic • Suitable for TPs engineered for FcRn binding at different pHs	• Redundant if FcRn engineering is not the focus of a study
Absorption Models		
Empirical model (first-order or saturable absorption)	• Simple • Sufficient for sparse data in the absorption phase	• Require data to inform model parameterization • Provides little information about the underlying mechanisms • Sometimes unable to capture data satisfactorily
Semimechanistic	• Characterize contribution of lymphatic versus blood absorption, lymphatic redistribution, and pre-systemic degradation • Provide more biologically meaningful parameter estimates • Compatible with compartmental or mPBPK models	• lack FcRn binding and other saturable transcellular processes • Bioavailability is assigned rather than predicted • Limited across-species translatability
Mechanistic	• Suitable in compartmental, mPBPK, and PBPK frameworks • Provide insights into various absorption mechanisms • Have better capability of interspecies scaling • Can guide dosing strategies	• Limited knowledge about the underlying physiology hinders model parameterization

were able to a priori predict subcutaneous PK of 3 out of 4 mAbs in the test dataset. Jones et al. (2019) also modeled the impact of molecular charge on mAb PK, using a somewhat different approach. Contrary to the predictor used in the model by Hu and D'Argenio (2020), PPC, which is theoretically calculated, this work used the data from affinity-capture self-interaction nanoparticle spectroscopy, an in vitro assay that detects nonspecific charge-based interactions as a covariate in the PBPK model. Instead of moderating the pinocytosis rate, the authors involved nonspecific binding between mAbs and cell membrane sites and internalization of the membrane-bound complex via pinocytosis. The nonspecific binding equilibrium constant was expressed as a function of scores from the in vitro assay, whereby greater self-association leading to higher binding affinity. After model calibration, mAb PK in mice and humans was predicted relatively well.

Modeling approaches incorporating the impact of glycosylation on mAb PK are less explored. This is in part due to inconsistent observations of the effect of high mannose (Kanda et al., 2007; Yu et al., 2012), hybrid type glycans (Kanda et al., 2007; Falck et al., 2021),

and galactosylation (Wright et al., 2000; Falck et al., 2021) on clearance. As glycoengineering of TPs gain more popularity, it can be expected that glycosylation will be an important covariate in PK models. As has been discussed in *Renal Elimination*, more data are needed to substantiate the relationship between molecular shape, charge, or rigidity and kidney elimination. Ultimately, a platform PBPK model incorporating physicochemical characteristics of TPs holds promise for predicting PK based on in silico and in vitro properties and guiding protein engineering strategies to achieve maximum and specific exposure at the site of action.

Modeling Next-Generation TPs. Innovative protein engineering technologies have paved the way for the generation of an array of novel TPs, which often possess unique physicochemical properties and mechanisms of action. Mechanistic models need to be evolved to understand determinants controlling their PK/PD and to aid in rational design of these next-generation modalities. Previous models may work well in capturing existent data, but novel molecules and unusual scenarios often require reexamination of model assumptions and refinement of model

TABLE 2

Examples of models that have been validated for cross-species or crosspopulation predictability of TPs' PK

Model Reference	Model Characteristics	Model Description/Application
Dong et al., 2011	Two-compartment model, allometric scaling	Prediction of linear plasma PK of mAbs following subcutaneous and subcutaneous administration in humans based on monkey PK data
Zhao et al., 2015	mPBPK, FcRn binding not included	Prediction of linear plasma PK of mAbs following subcutaneous administration in mice, rats, monkeys, and humans
Chen and Balthasar, 2012 Glassman et al., 2015 Glassman and Balthasar, 2016b	PBPK, TMDD (equilibrium binding), catenary endosomal model	Prediction of nonlinear plasma PK of mAbs in the presence of therapeutic targets across doses in mice, monkeys, and humans
Offman and Edginton, 2015 Offman et al., 2016	PBPK, one-pore	Prediction of subcutaneous PK of a pegylated peptide across dose levels in humans based on PK data following subcutaneous and subcutaneous administration in monkeys and one dose level of subcutaneous administration in humans
Chang et al., 2019	PBPK, kinetic FcRn binding, brain distribution submodel	Prediction of nontargeting mAb disposition in whole brain and CSF in mice, rats, monkeys, and humans
Shah and Betts, 2012 Chang et al., 2021a	PBPK, kinetic FcRn binding, age-dependent physiologic parameter values	Prediction of plasma PK of mAbs following intravenous administration in mice, rats, monkeys, human adults, and pediatric patients
Pan et al., 2020	PBPK, TMDD, two-pore, semimechanistic or first-order absorption model, age-dependent physiologic parameter values	Prediction of plasma PK of different-size TPs following intravenous or subcutaneous administration in full-term neonates, infants, children, adolescents, and adults
Khot et al., 2017	PBPK, tumor disposition model, allometric scaling	Prediction of plasma PK of different analytes of an ADC based on rat PK data

structures. Based on the types of modeling efforts required to elucidate the ADME mechanisms, these next-generation TPs can be roughly categorized into two nonexclusive groups.

The first group of TPs necessitate highly mechanistic cellular models to characterize intracellular processing, due to endosomal-environment switch mechanisms, or their intracellular-delivery nature. The well-known concept of "recycling antibodies" has been applied to IL-6R, IL-6, and PCSK 9, where antibodies bind tightly to the target extracellularly at pH 7.4 or with low calcium ion concentration and dissociate rapidly from the target in endosomes where pH is low or calcium ion is concentrated. These "catch-and-release" mAbs are expected to improve neutralization of soluble targets, and detailed modeling work has identified target turnover and pH-dependent binding affinity difference that maximize target clearance (Glassman and Balthasar, 2016a; Yang et al., 2017; Jones et al., 2020). The acid-switched binding is also of interest for membrane-bound targets (Kang et al., 2019), but relevant modeling analysis is scarce. ADCs are a class of drugs for which complex ADME properties have been extensively evaluated in PKPD models. Multiscale models have been developed to characterize systemic disposition and intracellular processing of the intact ADC, the antibody moiety, and the free drug (Maass et al., 2016; Khot et al., 2017; Singh and Shah, 2017a; Singh and Shah, 2017b; Singh et al., 2020). In recent years, biparatopic ADCs that recognize two nonoverlapping epitopes of the same target have gained much interest. Such constructs are believed to promote receptor clustering, inhibit receptor recycling, and promote lysosomal trafficking of the receptor and ADCs, thereby increasing cytotoxic drug release, as exemplified by biparatopic ADCs targeting HER2 (Li et al., 2016), MET (DaSilva et al., 2021), and EGFR (Fan et al., 2021). A mechanistic model can provide a quantitative understanding of the extent to which intracellular trafficking is altered, the resultant drug exposure improvement, and the long-term impact of receptor downregulation caused by clustering.

The second type of next-generation TPs use previously less-understood receptor-mediated disposition pathways. For example, exploiting transferrin receptor (TfR)-mediated transcytosis has been recognized as a strategy to enhance drug delivery across the BBB, as demonstrated using ADCs or bispecific mAbs targeting both TfR and therapeutic targets (Friden et al., 1991). Intriguingly, higher antibody exposure in the brain is observed when TfR engagement is monovalent or has only intermediate affinity (Yu et al., 2011; Niewoehner et al., 2014; Chang et al., 2021b), which ensures both sufficient TfR binding at the luminal side and efficient release to the abluminal side. Empirical and semimechanistic PKPD models have been explored to predict the optimal TfR affinity that maximizes brain exposure, as well as the impact on efficacy and safety (Gadkar et al., 2016; Kanodia et al., 2016). However, the influence of TfR binding valency has not been characterized, and translation of mouse and monkey models to human remains to be validated. Fc gamma receptor (FcγR)-mediated elimination represents another pathway that can play a role in TP disposition. FcγRs are known to be important in immune responses to mAbs, but their role in mAb PK is less defined. Although experiments with FcγR knockout mice suggested a minor role of FcγR in PK of a typical IgG1 molecule (Abuqayyas and Balthasar, 2012), for those TPs that can form large, high-order immune complexes with soluble ligands (Mortensen et al., 2012; Kasturirangan et al., 2017), or that have significant ADCC resulting in target cell depletion (Uchida et al., 2004), interaction with FcγRs may impact TP disposition. However, a systematic modeling analysis of this pathway is currently lacking. Another modality that falls in this category is albumin-fusion or albumin binding domain (ABD)-conjugated TPs, which leverages pH-dependent albumin-FcRn interactions to achieve half-life extension. This strategy has been applied to IgA (Meyer et al., 2016), single-chain diabodies (Stork et al., 2007), single-chain variable

fragments (Sanches et al., 2020), domain antibodies (Goodall et al., 2015), and affibodies (Andersen et al., 2011). A PBPK framework with the two-pore formalism has been demonstrated to well characterize PK of albumin, ABDs, and ABD-conjugated diabody (Sepp et al., 2019; Sepp et al., 2020). However, a more extensive evaluation of how the size of the unmodified TP and the size of the albumin-binding modality/albumin variants impact the half-life of TPs is still needed.

Conclusions

Mathematical and mechanistic PK models are crucial for the development of exposure-efficacy and exposure-toxicity relationships for TPs in preclinical species and humans. Here, we underscore the potential of PBPK modeling in characterizing unique ADME properties of TPs and demonstrate a diverse array of models with variable assumptions in describing transcapillary transport, tissue distribution, FcRn-mediated recycling, TMDD, renal elimination, and absorption. These models shed light on critical determinants influencing TPs' exposures in circulation or at the site of action and target engagement. We also highlight the emerging needs to integrate physicochemical properties of TPs in PK models to explain intermolecular PK variability and to elucidate novel disposition mechanisms of next-generation TPs using novel models. It is anticipated that the advanced PK models will facilitate triaging of TP candidates and optimization of molecular design. These quantitative tools can also facilitate model-informed discovery and development of biotherapeutics.

Authorship Contributions

Wrote or contributed to the writing of the manuscript: Liu, Shah.

References

Abuqayyas L and Balthasar JP (2012) Application of knockout mouse models to investigate the influence of FcγR on the tissue distribution and elimination of 8C2, a murine IgG1 monoclonal antibody. *Int J Pharm* **439**:8–16.

Akilesh S, Christianson GJ, Roopenian DC, and Shaw AS (2007) Neonatal FcR expression in bone marrow-derived cells functions to protect serum IgG from catabolism. *J Immunol* **179**: 4580–4588.

Andersen JT, Pehrson R, Tolmachev V, Daba MB, Abrahmsén L, and Ekblad C (2011) Extending half-life by indirect targeting of the neonatal Fc receptor (FcRn) using a minimal albumin binding domain. *J Biol Chem* **286**:5234–5241.

Arrowsmith J (2011) Trial watch: phase III and submission failures: 2007-2010. *Nat Rev Drug Discov* **10**:87.

Baxter LT, Zhu H, Mackensen DG, Butler WF, and Jain RK (1995) Biodistribution of monoclonal antibodies: scale-up from mouse to human using a physiologically based pharmacokinetic model. *Cancer Res* **55**:4611–4622.

Baxter LT, Zhu H, Mackensen DG, and Jain RK (1994) Physiologically based pharmacokinetic model for specific and nonspecific monoclonal antibodies and fragments in normal tissues and human tumor xenografts in nude mice. *Cancer Res* **54**:1517–1528.

Boswell CA, Ferl GZ, Mundo EE, Bumbaca D, Schweiger MG, Theil FP, Fielder PJ, and Khawli LA (2011) Effects of anti-VEGF on predicted antibody biodistribution: roles of vascular volume, interstitial volume, and blood flow. *PLoS One* **6**:e17874.

Boswell CA, Mundo EE, Ulufatu S, Bumbaca D, Cahaya HS, Majidy N, Van Hoy M, Schweiger MG, Fielder PJ, Prabhu S, et al. (2014) Comparative physiology of mice and rats: radiometric measurement of vascular parameters in rodent tissues. *Mol Pharm* **11**:1591–1598.

Boucher Y, Baxter LT, and Jain RK (1990) Interstitial pressure gradients in tissue-isolated and subcutaneous tumors: implications for therapy. *Cancer Res* **50**:4478–4484.

Bresler EH and Groome LJ (1981) On equations for combined convective and diffusive transport of neutral solute across porous membranes. *Am J Physiol* **241**:F469–F476.

Brinker T, Stopa E, Morrison J, and Klinge P (2014) A new look at cerebrospinal fluid circulation. *Fluids Barriers CNS* **11**:10.

Bumbaca Yadav D, Sharma VK, Boswell CA, Hotzel I, Tesar D, Shang Y, Ying Y, Fischer SK, Grogan JL, Chiang EY, et al. (2015) Evaluating the use of antibody variable region (Fv) charge as a risk assessment tool for predicting typical cynomolgus monkey pharmacokinetics. *J Biol Chem* **290**:29732–29741.

Bussing D and Shah DK (2020) Development of a physiologically-based pharmacokinetic model for ocular disposition of monoclonal antibodies in rabbits. *J Pharmacokinet Pharmacodyn* **47**:597–612.

Cao Y, Balthasar JP, and Jusko WJ (2013) Second-generation minimal physiologically-based pharmacokinetic model for monoclonal antibodies. *J Pharmacokinet Pharmacodyn* **40**:597–607.

Cao Y and Jusko WJ (2014) Incorporating target-mediated drug disposition in a minimal physiologically-based pharmacokinetic model for monoclonal antibodies. *J Pharmacokinet Pharmacodyn* **41**:375–387.

Challa DK, Wang X, Montoyo HP, Velmurugan R, Ober RJ, and Ward ES (2019) Neonatal Fc receptor expression in macrophages is indispensable for IgG homeostasis. *MAbs* **11**:848–860.

Chang HP, Shakhnovich V, Frymoyer A, Funk RS, Becker ML, Park KT, and Shah DK (2022) A population physiologically-based pharmacokinetic model to characterize antibody disposition in pediatrics and evaluation of the model using infliximab. *Br J Clin Pharmacol* **88**:290–302.

Chang HY, Wu S, Li Y, Zhang W, Burrell M, Webster CI, and Shah DK (2021b) Brain pharmacokinetics of anti-transferrin receptor antibody affinity variants in rats determined using microdialysis. *MAbs* **13**:1874121.

Chang HY, Wu S, Meno-Tetang G, and Shah DK (2019) A translational platform PBPK model for antibody disposition in the brain. *J Pharmacokinet Pharmacodyn* **46**:319–338.

Chen X, Hickling T, Kraynov E, Kuang B, Parng C, and Vicini P (2013) A mathematical model of the effect of immunogenicity on therapeutic protein pharmacokinetics. *AAPS J* **15**:1141–1154.

Chen X, Hickling TP, and Vicini P (2014a) A mechanistic, multiscale mathematical model of immunogenicity for therapeutic proteins: part 1-theoretical model. *CPT Pharmacometrics Syst Pharmacol* **3**:e133.

Chen X, Hickling TP, and Vicini P (2014b) A mechanistic, multiscale mathematical model of immunogenicity for therapeutic proteins: part 2-model applications. *CPT Pharmacometrics Syst Pharmacol* **3**:e134.

Chen X, Jiang X, Doddareddy R, Geist B, McIntosh T, Jusko WJ, Zhou H, and Wang W (2018) Development and Translational Application of a Minimal Physiologically Based Pharmacokinetic Model for a Monoclonal Antibody against Interleukin 23 (IL-23) in IL-23-Induced Psoriasis-Like Mice. *J Pharmacol Exp Ther* **365**:140–155.

Chen Y and Balthasar JP (2012) Evaluation of a catenary PBPK model for predicting the in vivo disposition of mAbs engineered for high-affinity binding to FcRn. *AAPS J* **14**:850–859.

Chung SW, Hil-lal TA, and Byun Y (2012) Strategies for non-invasive delivery of biologics. *J Drug Target* **20**:481–501.

Cilliers C, Guo H, Liao J, Christodolu N, and Thurber GM (2016) Multiscale modeling of antibody-drug conjugates: connecting tissue and cellular distribution to whole animal pharmacokinetics and potential implications for efficacy. *AAPS J* **18**:1117–1130.

Collins DS, Sánchez-Félix M, Badkar AV, and Mrsny R (2020) Accelerating the development of novel technologies and tools for the subcutaneous delivery of biotherapeutics. *J Control Release* **321**:475–482.

Conner KP, Devanaboyina SC, Thomas VA, and Rock DA (2020) The biodistribution of therapeutic proteins: Mechanism, implications for pharmacokinetics, and methods of evaluation. *Pharmacol Ther* **212**:107574.

Covell DG, Barbet J, Holton OD, Black CD, Parker RJ, and Weinstein JN (1986) Pharmacokinetics of monoclonal immunoglobulin G1, F(ab')2, and Fab' in mice. *Cancer Res* **46**:3969–3978.

DaSilva JO, Yang K, Surriga O, Nittoli T, Kunz A, Franklin MC, Delfino FJ, Mao S, Zhao F, Giurleo JT, et al. (2021) A Biparatopic Antibody-Drug Conjugate to Treat MET-Expressing Cancers, Including Those that Are Unresponsive to MET Pathway Blockade. *Mol Cancer Ther* **20**:1966–1976.

Datta-Mannan A, Thangaraju A, Leung D, Tang Y, Witcher DR, Lu J, and Wroblewski VJ (2015) Balancing charge in the complementarity-determining regions of humanized mAbs without affecting pI reduces non-specific binding and improves the pharmacokinetics. *MAbs* **7**:483–493.

Davda JP, Jain M, Batra SK, Gwilt PR, and Robinson DH (2008) A physiologically based pharmacokinetic (PBPK) model to characterize and predict the disposition of monoclonal antibody CC49 and its single chain Fv constructs. *Int Immunopharmacol* **8**:401–413.

Deng R, Meng YG, Hoyte K, Lutman J, Lu Y, Iyer S, DeForge LE, Theil FP, Fielder PJ, and Prabhu S (2012) Subcutaneous bioavailability of therapeutic antibodies as a function of FcRn binding affinity in mice. *MAbs* **4**:101–109.

Dong JQ, Salinger DH, Endres CJ, Gibbs JP, Hsu CP, Stouch BJ, Hurh E, and Gibbs MA (2011) Quantitative prediction of human pharmacokinetics for monoclonal antibodies: retrospective analysis of monkey as a single species for first-in-human prediction. *Clin Pharmacokinet* **50**:131–142.

Falck B, Thomann M, Lechmann M, Koeleman CAM, Malik S, Jany C, Wuhrer M, and Reusch D (2021) Glycoform-resolved pharmacokinetic studies in a rat model employing glycoengineered variants of a therapeutic monoclonal antibody. *MAbs* **13**:1865596.

Fan J, Zhuang X, Yang X, Xu Y, Zhou Z, Pan L, and Chen S (2021) A multivalent biparatopic EGFR-targeting nanobody drug conjugate displays potent anticancer activity in solid tumor models. *Signal Transduct Target Ther* **6**:320.

Ferl GZ, Theil FP, and Wong H (2016) Physiologically based pharmacokinetic models of small molecules and therapeutic antibodies: a mini-review on fundamental concepts and applications. *Biopharm Drug Dispos* **37**:75–92.

Ferl GZ, Wu AM, and DiStefano 3rd JJ (2005) A predictive model of therapeutic monoclonal antibody dynamics and regulation by the neonatal Fc receptor (FcRn). *Ann Biomed Eng* **33**: 1640–1652.

Friden PM, Walus LR, Musso GF, Taylor MA, Malfroy B, and Starzyk RM (1991) Anti-transferrin antibody and antibody-drug conjugates cross the blood-brain barrier. *Proc Natl Acad Sci USA* **88**:4771–4775.

Fujimori K, Covell DG, Fletcher JE, and Weinstein JN (1990) A modeling analysis of monoclonal antibody percolation through tumors: a binding-site barrier. *J Nucl Med* **31**:1191–1198.

Gadkar K, Yadav DB, Zuchero JY, Couch JA, Kanodia J, Kenrick MK, Atwal JK, Dennis MS, Prabhu S, Watts RJ, et al. (2016) Mathematical PKPD and safety model of bispecific TfR/BACE1 antibodies for the optimization of antibody uptake in brain. *Eur J Pharm Biopharm* **101**:53–61.

Gaohua L, Wedagedera J, Small BG, Almond L, Romero K, Hermann D, Hanna D, Jamei M, and Gardner I (2015) Development of a Multicompartment Permeability-Limited Lung PBPK Model and Its Application in Predicting Pulmonary Pharmacokinetics of Antituberculosis Drugs. *CPT Pharmacometrics Syst Pharmacol* **4**:605–613.

Garg A and Balthasar JP (2007) Physiologically-based pharmacokinetic (PBPK) model to predict IgG tissue kinetics in wild-type and FcRn-knockout mice. *J Pharmacokinet Pharmacodyn* **34**:687–709.

Germovsek E, Cheng M, and Giragossian C (2021) Allometric scaling of therapeutic monoclonal antibodies in preclinical and clinical settings. *MAbs* **13**:1964935.

Gibbs JP, Yuraszeck T, Biesdorf C, Xu Y, and Kasichayanula S (2020) Informing Development of Bispecific Antibodies Using Physiologically Based Pharmacokinetic-Pharmacodynamic Models: Current Capabilities and Future Opportunities. *J Clin Pharmacol* **60** (Suppl 1):S132–S146.

Gibiansky L and Frey N (2012) Linking interleukin-6 receptor blockade with tocilizumab and its hematological effects using a modeling approach. *J Pharmacokinet Pharmacodyn* **39**:5–16.

Gibiansky L and Gibiansky E (2014) Target-mediated drug disposition model and its approximations for antibody-drug conjugates. *J Pharmacokinet Pharmacodyn* **41**:35–47.

Gibiansky L, Gibiansky E, Kakkar T, and Ma P (2008) Approximations of the target-mediated drug disposition model and identifiability of model parameters. *J Pharmacokinet Pharmacodyn* **35**:573–591.

Gill KL, Gardner I, Li L, and Jamei M (2016) A Bottom-Up Whole-Body Physiologically Based Pharmacokinetic Model to Mechanistically Predict Tissue Distribution and the Rate of Subcutaneous Absorption of Therapeutic Proteins. *AAPS J* **18**:156–170.

Glassman PM and Balthasar JP (2016a) Application of a catenary PBPK model to predict the disposition of "catch and release" anti-PCSK9 antibodies. *Int J Pharm* **505**:69–78.

Glassman PM and Balthasar JP (2016b) Physiologically-based pharmacokinetic modeling to predict the clinical pharmacokinetics of monoclonal antibodies. *J Pharmacokinet Pharmacodyn* **43**:427–446.

Glassman PM and Balthasar JP (2019) Physiologically-based modeling of monoclonal antibody pharmacokinetics in drug discovery and development. *Drug Metab Pharmacokinet* **34**:3–13.

Glassman PM, Chen Y, and Balthasar JP (2015) Scale-up of a physiologically-based pharmacokinetic model to predict the disposition of monoclonal antibodies in monkeys. *J Pharmacokinet Pharmacodyn* **42**:527–540.

Goodall LJ, Ovecka M, Rycroft D, Friel SL, Sanderson A, Mistry P, Davies ML, and Stoop AA (2015) Pharmacokinetic and Pharmacodynamic Characterisation of an Anti-Mouse TNF Receptor 1 Domain Antibody Formatted for In Vivo Half-Life Extension. *PLoS One* **10**:e0137065.

Grotte G (1956) Passage of dextran molecules across the blood-lymph barrier. *Acta Chir Scand Suppl* **211**:1–84.

Haraldsson B, Nyström J, and Deen WM (2008) Properties of the glomerular barrier and mechanisms of proteinuria. *Physiol Rev* **88**:451–487.

Hay M, Thomas DW, Craighead JL, Economides C, and Rosenthal J (2014) Clinical development success rates for investigational drugs. *Nat Biotechnol* **32**:40–51.

Hu S and D'Argenio DZ (2020) Predicting monoclonal antibody pharmacokinetics following subcutaneous administration via whole-body physiologically-based modeling. *J Pharmacokinet Pharmacodyn* **47**:385–409.

Ibrahim R, Nitsche JM, and Kasting GB (2012) Dermal clearance model for epidermal bioavailability calculations. *J Pharm Sci* **101**:2094–2108.

Jones HM, Tolsma J, Zhang Z, Jasper P, Luo H, Weber GL, Wright K, Bard J, Bell R, Messing D, et al. (2020) A Physiologically-Based Pharmacokinetic Model for the Prediction of "Half-Life Extension" and "Catch and Release" Monoclonal Antibody Pharmacokinetics. *CPT Pharmacometrics Syst Pharmacol* **9**:534–541.

Jones HM, Zhang Z, Jasper P, Luo H, Avery LB, King LE, Neubert H, Barton HA, Betts AM, and Webster R (2019) A Physiologically-Based Pharmacokinetic Model for the Prediction of Monoclonal Antibody Pharmacokinetics From In Vitro Data. *CPT Pharmacometrics Syst Pharmacol* **8**:738–747.

Kagan L (2014) Pharmacokinetic modeling of the subcutaneous absorption of therapeutic proteins. *Drug Metab Dispos* **42**:1890–1905.

Kagan L, Gershkovich P, Mendelman A, Amsili S, Ezov N, and Hoffman A (2007) The role of the lymphatic system in subcutaneous absorption of macromolecules in the rat model. *Eur J Pharm Biopharm* **67**:759–765.

Kanda Y, Yamada T, Mori K, Okazaki A, Inoue M, Kitajima-Miyama K, Kuni-Kamochi R, Nakano R, Yano K, Kakita S et al. (2007) Comparison of biological activity among nonfucosylated therapeutic IgG1 antibodies with three different N-linked Fc oligosaccharides: the high-mannose, hybrid, and complex types. *Glycobiology* **17**:104–118.

Kang JC, Sun W, Khare P, Karimi M, Wang X, Shen Y, Ober RJ, and Ward ES (2019) Engineering a HER2-specific antibody-drug conjugate to increase lysosomal delivery and therapeutic efficacy. *Nat Biotechnol* **37**:523–526.

Kanodia JS, Gadkar K, Bumbaca D, Zhang Y, Tong RK, Luk W, Hoyte K, Lu Y, Wildsmith KR, Couch JA, et al. (2016) Prospective Design of Anti-Transferrin Receptor Bispecific Antibodies for Optimal Delivery into the Human Brain. *CPT Pharmacometrics Syst Pharmacol* **5**:283–291.

Kasturirangan S, Rainey GJ, Xu L, Wang X, Portnoff A, Chen T, Fazenbaker C, Zhong H, Bee J, Zeng Z, et al. (2017) Targeted Fcγ Receptor (FcγR)-mediated Clearance by a Biparatopic Bispecific Antibody. *J Biol Chem* **292**:4361–4370.

Kathman Jr S, Thway TM, Zhou L, Lee S, Yu S, Ma M, Chirmule N, and Jawa V (2016) Utility of a Bayesian Mathematical Model to Predict the Impact of Immunogenicity on Pharmacokinetics of Therapeutic Proteins. *AAPS J* **18**:424–431.

Khot A, Tibbitts J, Rock D, and Shah DK (2017) Development of a Translational Physiologically Based Pharmacokinetic Model for Antibody-Drug Conjugates: a Case Study with T-DM1. *AAPS J* **19**:1715–1734.

Kola I and Landis J (2004) Can the pharmaceutical industry reduce attrition rates? *Nat Rev Drug Discov* **3**:711–715.

Kuang B, King L, and Wang HF (2010) Therapeutic monoclonal antibody concentration monitoring: free or total? *Bioanalysis* **2**:1125–1140.

Lagassé HA, Alexaki A, Simhadri VL, Katagiri NH, Jankowski W, Sauna ZE, and Kimchi-Sarfaty C (2017) Recent advances in (therapeutic protein) drug development. *F1000 Res* **6**:113.

Latvala S, Jacobsen B, Otteneder MB, Herrmann A, and Kronenberg S (2017) Distribution of FcRn Across Species and Tissues. *J Histochem Cytochem* **65**:321–333.

Lavezzi SM, Mezzalana E, Zamuner S, De Nicolao G, Ma P, and Simeoni M (2018) MPBPK-TMDD models for mAbs: alternative models, comparison, and identifiability issues. *J Pharmacokinet Pharmacodyn* **45**:787–802.

Levy G (1994) Pharmacologic target-mediated drug disposition. *Clin Pharmacol Ther* **56**:248–252.

Li JY, Perry SR, Muniz-Medina V, Wang X, Wetzel LK, Rebelatto MC, Hinrichs MJ, Bezabeh BZ, Fleming RL, Dimasi N, et al. (2016) A Biparatopic HER2-Targeting Antibody-Drug Conjugate Induces Tumor Regression in Primary Models Refractory to or Ineligible for HER2-Targeted Therapy. *Cancer Cell* **29**:117–129.

Li L, Gardner I, Rose R, and Jamei M (2014) Incorporating Target Shedding Into a Minimal PBPK-TMDD Model for Monoclonal Antibodies. *CPT Pharmacometrics Syst Pharmacol* **3**:e96.

Li T and Balthasar JP (2018) FcRn Expression in Wildtype Mice, Transgenic Mice, and in Human Tissues. *Biomolecules* **8**:115.

Li T and Balthasar JP (2019) Application of Physiologically Based Pharmacokinetic Modeling to Predict the Effects of FcRn Inhibitors in Mice, Rats, and Monkeys. *J Pharm Sci* **108**:701–713.

Li Z and Shah DK (2019) Two-pore physiologically based pharmacokinetic model with de novo derived parameters for predicting plasma PK of different size protein therapeutics. *J Pharmacokinet Pharmacodyn* **46**:305–318.

Li Z, Yu X, Li Y, Verma A, Chang HP, and Shah DK (2021) A Two-Pore Physiologically Based Pharmacokinetic Model to Predict Subcutaneously Administered Different-Size Antibody/Antibody Fragments. *AAPS J* **23**:62.

Liang W, Pan HW, Vllasaliu D, and Lam JKW (2020) Pulmonary Delivery of Biological Drugs. *Pharmaceutics* **12**:1025.

Lobo ED, Hansen RJ, and Balthasar JP (2004) Antibody pharmacokinetics and pharmacodynamics. *J Pharm Sci* **93**:2645–2668.

Maass KF, Kulkarni C, Betts AM, and Wittrup KD (2016) Determination of Cellular Processing Rates for a Trastuzumab-Maytansinoid Antibody-Drug Conjugate (ADC) Highlights Key Parameters for ADC Design. *AAPS J* **18**:635–646.

Mach H, Gregory SM, Mackiewicz A, Mittal S, Lalloo A, Kirchmeier M, and Shameem M (2011) Electrostatic interactions of monoclonal antibodies with subcutaneous tissue. *Ther Deliv* **2**:727–736.

Mager DE and Jusko WJ (2001) General pharmacokinetic model for drugs exhibiting target-mediated drug disposition. *J Pharmacokinet Pharmacodyn* **28**:507–532.

Mager DE and Krzyzanski W (2005) Quasi-equilibrium pharmacokinetic model for drugs exhibiting target-mediated drug disposition. *Pharm Res* **22**:1589–1596.

Malik PRV and Edginton AN (2020) Integration of Ontogeny Into a Physiologically Based Pharmacokinetic Model for Monoclonal Antibodies in Premature Infants. *J Clin Pharmacol* **60**:466–476.

Malik PRV, Hamadeh A, Phipps C, and Edginton AN (2017) Population PBPK modelling of trastuzumab: a framework for quantifying and predicting inter-individual variability. *J Pharmacokinet Pharmacodyn* **44**:277–290.

Mandikian D, Figueroa I, Oldendorp A, Rafidi H, Ulufatu S, Schweiger MG, Couch JA, Dybdal N, Joseph SB, Prabhu S, et al. (2018) Tissue Physiology of Cynomolgus Monkeys: Cross-Species Comparison and Implications for Translational Pharmacology. *AAPS J* **20**:107.

Marathe A, Krzyzanski W, and Mager DE (2009) Numerical validation and properties of a rapid binding approximation of a target-mediated drug disposition pharmacokinetic model. *J Pharmacokinet Pharmacodyn* **36**:199–219.

McDonald TA, Zepeda ML, Tomlinson MJ, Bee WH, and Ivens IA (2010) Subcutaneous administration of biotherapeutics: current experience in animal models. *Curr Opin Mol Ther* **12**:461–470.

Meibohm B and Zhou H (2012) Characterizing the impact of renal impairment on the clinical pharmacology of biologics. *J Clin Pharmacol* **52**(1, Suppl)54S–62S.

Meyer S, Nederend M, Jansen JH, Reiding KR, Jacobino SR, Meeldijk J, Bovenschen N, Wuhrer M, Valerius T, Ubink R, et al. (2016) Improved in vivo anti-tumor effects of IgA-Her2 antibodies through half-life extension and serum exposure enhancement by FcRn targeting. *MAbs* **8**:87–98.

Montoyo HP, Vaccaro C, Hafner M, Ober RJ, Mueller W, and Ward ES (2009) Conditional deletion of the MHC class I-related receptor FcRn reveals the sites of IgG homeostasis in mice. *Proc Natl Acad Sci USA* **106**:2788–2793.

Morgan P, Van Der Graaf PH, Arrowsmith J, Feltner DE, Drummond KS, Wegner CD, and Street SD (2012) Can the flow of medicines be improved? Fundamental pharmacokinetic and pharmacological principles toward improving Phase II survival. *Drug Discov Today* **17**:419–424.

Mortensen DL, Prabhu S, Stefanich EG, Kadkhodayan-Fischer S, Gelzleichter TR, Baker D, Jiang J, Wallace K, Iyer S, Fielder PJ, et al. (2012) Effect of antigen binding affinity and effector function on the pharmacokinetics and pharmacodynamics of anti-IgE monoclonal antibodies. *MAbs* **4**:724–731.

Mullard A (2021) FDA approves 100th monoclonal antibody product. *Nat Rev Drug Discov* **20**:491–495.

Ng CM, Bruno R, Combs D, and Davies B (2005) Population pharmacokinetics of rituximab (anti-CD20 monoclonal antibody) in rheumatoid arthritis patients during a phase II clinical trial. *J Clin Pharmacol* **45**:792–801.

Niederalt C, Kuepfer L, Solodenko J, Eissing T, Siegmund HU, Block M, Willmann S, and Lippert J (2018) A generic whole body physiologically based pharmacokinetic model for therapeutic proteins in PK-Sim. *J Pharmacokinet Pharmacodyn* **45**:235–257.

Niewoehner J, Bohrmann B, Collin L, Urich E, Sade H, Maier P, Rueger P, Stracke JO, Lau W, Tissot AC, et al. (2014) Increased brain penetration and potency of a therapeutic antibody using a monovalent molecular shuttle. *Neuron* **81**:49–60.

Ober RJ, Radu CG, Ghetie V, and Ward ES (2001) Differences in promiscuity for antibody-FcRn interactions across species: implications for therapeutic antibodies. *Int Immunol* **13**:1551–1559.

Offman E and Edginton AN (2015) A PBPK workflow for first-in-human dose selection of a subcutaneously administered pegylated peptide. *J Pharmacokinet Pharmacodyn* **42**:135–150.

Offman E, Phipps C, and Edginton AN (2016) Population physiologically-based pharmacokinetic model incorporating lymphatic uptake for a subcutaneously administered pegylated peptide. *In Silico Pharmacol* **4**:3.

Pan X, Stader F, Abduljalil K, Gill KL, Johnson TN, Gardner I, and Jamei M (2020) Development and Application of a Physiologically-Based Pharmacokinetic Model to Predict the Pharmacokinetics of Therapeutic Proteins from Full-term Neonates to Adolescents. *AAPS J* **22**:76.

Patton JS, Brain JD, Davies LA, Fiegel J, Gumbleton M, Kim KJ, Sakagami M, Vanbever R, and Ehrhardt C (2010) The particle has landed–characterizing the fate of inhaled pharmaceuticals. *J Aerosol Med Pulm Drug Deliv* **23** (Suppl 2):S71–S87.

Patton JS and Byron PR (2007) Inhaling medicines: delivering drugs to the body through the lungs. *Nat Rev Drug Discov* **6**:67–74.

Peletier LA and Gabrielsson J (2018) New Equilibrium Models of Drug-Receptor Interactions Derived from Target-Mediated Drug Disposition. *AAPS J* **20**:69.

Perez Ruixo JJ, Ma P, and Chow AT (2013) The utility of modeling and simulation approaches to evaluate immunogenicity effect on the therapeutic protein pharmacokinetics. *AAPS J* **15**:172–182.

Perez VL, Saeed AM, Tan Y, Urbieta M, and Cruz-Guilloty F (2013) The eye: A window to the soul of the immune system. *J Autoimmun* **45**:7–14.

Porter CJ and Charman SA (2000) Lymphatic transport of proteins after subcutaneous administration. *J Pharm Sci* **89**:297–310.

Porter CJ, Edwards GA, and Charman SA (2001) Lymphatic transport of proteins after s.c. injection: implications of animal model selection. *Adv Drug Deliv Rev* **50**:157–171.

Rabkin R and Dahl DC (1993) Renal uptake and disposal of proteins and peptides, in *Biological Barriers to Protein Delivery* (Audus KL and Raub TJ, eds) pp 299–338, Springer.

Rafidi H, Estevez A, Ferl GZ, Mandikian D, Stainton S, Sermeño L, Williams SP, Kamath AV, Koerber JT, and Boswell CA (2021) Imaging Reveals Importance of Shape and Flexibility for Glomerular Filtration of Biologics. *Mol Cancer Ther* **20**:2008–2015.

Reddy ST, Berk DA, Jain RK, and Swartz MA (1985) A sensitive in vivo model for quantifying interstitial convective transport of injected macromolecules and nanoparticles. *J Appl Physiol* **101:**1162–1169.

Richter WF, Christianson GJ, Frances N, Grimm HP, Proetzel G, and Roopenian DC (2018) Hematopoietic cells as site of first-pass catabolism after subcutaneous dosing and contributors to systemic clearance of a monoclonal antibody in mice. *MAbs* **10:**803–813.

Richter WF and Jacobsen B (2014) Subcutaneous absorption of biotherapeutics: knowns and unknowns. *Drug Metab Dispos* **42:**1881–1889.

Rippe B and Haraldsson B (1987) Fluid and protein fluxes across small and large pores in the microvasculature. Application of two-pore equations. *Acta Physiol Scand* **131:**411–428.

Rippe B and Haraldsson B (1994) Transport of macromolecules across microvascular walls: the two-pore theory. *Physiol Rev* **74:**163–219.

Sanches M, D'Angelo I, Jaramillo M, Baardsnes J, Zwaagstra J, Schrag J, Schoenhofen I, Acchione M, Lawn S, Wickman G, et al. (2020) AlbuCORE: an albumin-based molecular scaffold for multivalent biologics design. *MAbs* **12:**1802188.

Sánchez-Félix M, Burke M, Chen HH, Patterson C, and Mittal S (2020) Predicting bioavailability of monoclonal antibodies after subcutaneous administration: Open innovation challenge. *Adv Drug Deliv Rev* **167:**66–77.

Schmidt MM and Wittrup KD (2009) A modeling analysis of the effects of molecular size and binding affinity on tumor targeting. *Mol Cancer Ther* **8:**2861–2871.

Sepp A, Berges A, Sanderson A, and Meno-Tetang G (2015) Development of a physiologically based pharmacokinetic model for a domain antibody in mice using the two-pore theory. *J Pharmacokinet Pharmacodyn* **42:**97–109.

Sepp A, Bergström M, and Davies M (2020) Cross-species/cross-modality physiologically based pharmacokinetics for biologics: 89Zr-labelled albumin-binding domain antibody GSK3128349 in humans. *MAbs* **12:**1832861.

Sepp A, Meno-Tetang G, Weber A, Sanderson A, Schon O, and Berges A (2019) Computer-assembled cross-species/cross-modalities two-pore physiologically based pharmacokinetic model for biologics in mice and rats. *J Pharmacokinet Pharmacodyn* **46:**339–359.

Shah DK (2015) Pharmacokinetic and pharmacodynamic considerations for the next generation protein therapeutics. *J Pharmacokinet Pharmacodyn* **42:**553–571.

Shah DK and Betts AM (2012) Towards a platform PBPK model to characterize the plasma and tissue disposition of monoclonal antibodies in preclinical species and human. *J Pharmacokinet Pharmacodyn* **39:**67–86.

Shah DK, Shin BS, Veith J, Tóth K, Bernacki RJ, and Balthasar JP (2009) Use of an anti-vascular endothelial growth factor antibody in a pharmacokinetic strategy to increase the efficacy of intraperitoneal chemotherapy. *J Pharmacol Exp Ther* **329:**580–591.

Singh AP, Seigel GM, Guo L, Verma A, Wong GG, Cheng HP, and Shah DK (2020) Evolution of the Systems Pharmacokinetics-Pharmacodynamics Model for Antibody-Drug Conjugates to Characterize Tumor Heterogeneity and *In Vivo* Bystander Effect. *J Pharmacol Exp Ther* **374:**184–199.

Singh AP and Shah DK (2017a) Application of a PK-PD Modeling and Simulation-Based Strategy for Clinical Translation of Antibody-Drug Conjugates: a Case Study with Trastuzumab Emtansine (T-DM1). *AAPS J* **19:**1054–1070.

Singh AP and Shah DK (2017b) Measurement and Mathematical Characterization of Cell-Level Pharmacokinetics of Antibody-Drug Conjugates: A Case Study with Trastuzumab-vc-MMAE. *Drug Metab Dispos* **45:**1120–1132.

Stork R, Müller D, and Kontermann RE (2007) A novel tri-functional antibody fusion protein with improved pharmacokinetic properties generated by fusing a bispecific single-chain diabody with an albumin-binding domain from streptococcal protein G. *Protein Eng Des Sel* **20:**569–576.

Thurber GM, Schmidt MM, and Wittrup KD (2008) Antibody tumor penetration: transport opposed by systemic and antigen-mediated clearance. *Adv Drug Deliv Rev* **60:**1421–1434.

Thurber GM and Wittrup KD (2012) A mechanistic compartmental model for total antibody uptake in tumors. *J Theor Biol* **314:**57–68.

Uchida J, Hamaguchi Y, Oliver JA, Ravetch JV, Poe JC, Haas KM, and Tedder TF (2004) The innate mononuclear phagocyte network depletes B lymphocytes through Fc receptor-dependent mechanisms during anti-CD20 antibody immunotherapy. *J Exp Med* **199:**1659–1669.

Urquhart L (2021) Top companies and drugs by sales in 2020. *Nat Rev Drug Discov* **20:**253.

Urva SR, Yang VC, and Balthasar JP (2010) Physiologically based pharmacokinetic model for T84.66: a monoclonal anti-CEA antibody. *J Pharm Sci* **99:**1582–1600.

Vidarsson G, Stemerding AM, Stapleton NM, Spliethoff SE, Janssen H, Rebers FE, de Haas M, and van de Winkel JG (2006) FcRn: an IgG receptor on phagocytes with a novel role in phagocytosis. *Blood* **108:**3573–3579.

Vugmeyster Y, Xu X, Theil FP, Khawli LA, and Leach MW (2012) Pharmacokinetics and toxicology of therapeutic proteins: Advances and challenges. *World J Biol Chem* **3:**73–92.

Wang W, Wang EQ, and Balthasar JP (2008) Monoclonal antibody pharmacokinetics and pharmacodynamics. *Clin Pharmacol Ther* **84:**548–558.

Wienkers LC and Heath TG (2005) Predicting in vivo drug interactions from in vitro drug discovery data. *Nat Rev Drug Discov* **4:**825–833.

Wright A, Sato Y, Okada T, Chang K, Endo T, and Morrison S (2000) In vivo trafficking and catabolism of IgG1 antibodies with Fc associated carbohydrates of differing structure. *Glycobiology* **10:**1347–1355.

Yang D, Giragossian C, Castellano S, Lasaro M, Xiao H, Saraf H, Hess Kenny C, Rybina I, Huang ZF, Ahlberg J, et al. (2017) Maximizing in vivo target clearance by design of pH-dependent target binding antibodies with altered affinity to FcRn. *MAbs* **9:**1105–1117.

Yu M, Brown D, Reed C, Chung S, Lutman J, Stefanich E, Wong A, Stephan JP, and Bayer R (2012) Production, characterization, and pharmacokinetic properties of antibodies with N-linked mannose-5 glycans. *MAbs* **4:**475–487.

Yu YJ, Zhang Y, Kenrick M, Hoyte K, Luk W, Lu Y, Atwal J, Elliott JM, Prabhu S, Watts RJ, et al. (2011) Boosting brain uptake of a therapeutic antibody by reducing its affinity for a transcytosis target. *Sci Transl Med* **3:**84ra44.

Yu YR, O'Koren EG, Hotten DF, Kan MJ, Kopin D, Nelson ER, Que L, and Gunn MD (2016) A Protocol for the Comprehensive Flow Cytometric Analysis of Immune Cells in Normal and Inflamed Murine Non-Lymphoid Tissues. *PLoS One* **11:**e0150606.

Zhao J, Cao Y, and Jusko WJ (2015) Across-Species Scaling of Monoclonal Antibody Pharmacokinetics Using a Minimal PBPK Model. *Pharm Res* **32:**3269–3281.

Zhao L, Ji P, Li Z, Roy P, and Sahajwalla CG (2013) The antibody drug absorption following subcutaneous or intramuscular administration and its mathematical description by coupling physiologically based absorption process with the conventional compartment pharmacokinetic model. *J Clin Pharmacol* **53:**314–325.

Zheng Y, Tesar DB, Benincosa L, Birnböck H, Boswell CA, Bumbaca D, Cowan KJ, Danilenko DM, Daugherty AL, Fielder PJ, et al. (2012) Minipig as a potential translatable model for monoclonal antibody pharmacokinetics after intravenous and subcutaneous administration. *MAbs* **4:**243–255.

Address Correspondence to: Dr. Dhaval K. Shah, 455 Pharmacy Building, Buffalo, NY 14214. E-mail: dshah4@buffalo.edu